ELSEVIER

Polymer 43 (2002) 3001–3006

polymer

www.elsevier.com/locate/polymer

Interfacial tension measurement between immiscible polymers: improved deformed drop retraction method

Younggon Son, Kalman B. Migler*

Polymer Division, NIST, 100 Bureau Dr., Gaithersburg, MD 20899-8542, USA

Received 15 October 2001; received in revised form 22 January 2002; accepted 24 January 2002

Abstract

This paper describes an improvement of the technique to measure interfacial tension in immiscible polymer blends. Our method is based on the droplet retraction method, in which one relates the kinetics of relaxation of a deformed droplet to the interfacial tension between the matrix and droplet. Previously, the problem with this technique has been the difficulty in preparing axisymmetric ellipsoidal droplets. In our work, we demonstrate that perfect axisymmetric ellipsoidal droplets are produced at a later stage of relaxation of short imbedded fibers. With this technique, we utilize the strengths of both the deformed droplet method and the imbedded fiber retraction method while overcoming their shortcomings. The interfacial tension value thus obtained was compared to that by conventional methods. Additionally, the effect of confinement by external walls on the interfacial tension measurement was studied. Confinement affects interfacial tension measurement when the gap between the walls is less than two times the equilibrium drop size.

Keywords: Deformed drop retraction method; Imbedded fiber retraction method; Interfacial tension

1. Introduction

It is well known that the interfacial tension between immiscible polymers in a blend is a critical factor for the morphology and final properties of the blend [1,2]. The numerous applications of polymer blends have lead to demand for methods to measure the interfacial tension between polymer pairs with greater accuracy and convenience. Many attempts have been made to develop accurate and convenient techniques to measure the interfacial tension for polymers.

Early attempts adopted the conventional methods for low viscosity materials, such as the pendant drop [3–5], the sessile drop [6], and the spinning drop [7,8]. In these methods, the interfacial tension is obtained by measuring the shape of the liquid–liquid interface, when the interfacial force is equilibrated by external forces such as gravity and the centrifugal force. They all require the accurate measurement of the density difference between the two liquids. In many cases, the density difference between two polymers is very small, which limits the accuracy of the interfacial tension measurement. Additionally, due to the high viscosity of polymeric materials, the equilibrium time is very long, which risks thermal degradation.

Dynamic methods can overcome those limitations. In these methods, the interfacial tension is obtained by observing the shape evolution of the interface. Several methods, such as the breaking thread (BT) [9–12], imbedded fiber retraction (IFR) [13–16] and deformed drop retraction (DDR) [17] have been developed. The BT method is based on Tomotika's equation [18], which describes the capillary instability and disintegration of a long liquid cylinder surrounded by another fluid. In order to obtain useful results, a perfect sinusoidal distortion of the interface is required. The length to diameter ratio must be greater than 60 and the diameter must be spatially constant. These requirements are not easy to attain in practical experiments [10]. Otherwise, thread retraction, end pinching and distortion growth at irregular wavelengths occur. The IFR method was first developed by Carriere and co-workers [13–15]. They modeled a short fiber as a cylinder capped with two hemispheres and expressed a governing equation from a macroscopic force balance between viscous dissipation and decrease in free energy of the interface in a somewhat ad hoc manner. This method overcomes the limitation encountered in the BT method and allows easier sample preparation, but requires empirical parameters of the mathematical model estimated by best fitting to experimental data for a system of known interfacial tension.

* Corresponding author.

E-mail addresses: sonyg@nist.gov (Y. Son), kalman.migler@nist.gov (K.B. Migler).

0032-3861/02/$ - see front matter
PII: S0032-3861(02)00097-6

Most recently, Luciani et al. [17] introduced a new method which can overcome the limitations described earlier. They measured the interfacial tension by observing the shape evolution of a drop initially deformed by an external shear force. From a general equation derived by Rallison [19], they derived the following theoretical equation describing the shape evolution of an ellipsoidal liquid drop suspended in an infinite fluid domain upon cessation of the flow

$$D = D_0 \exp\left\{-\frac{40(p+1)}{(2p+3)(19p+16)}\frac{\sigma}{\eta_m R_0}t\right\} \quad (1)$$

where D is the drop deformation parameter defined as $D = (L-B)/(L+B)$, where L and B are the major and minor axis of the ellipsoidal drop, respectively. D_0 is an initial deformation parameter, σ the interfacial tension, η_m the viscosity of the matrix phase, R_0 a radius of the drop at an equilibrium, p the viscosity ratio, and t is time. This equation is valid only for axisymmetrical ellipsoidal drops ($B = W$, W is the other minor axis). Luciani et al. applied shear stress to deform the drops. However, the B and W of a sheared drop in fluid are generally not the same due to the normal stresses in the droplet and/or matrix [20–25]. Though B and W may approach the same value before the drop becomes spherical (depending on the applied shear force) [21,22], one cannot avoid large relative errors in L and B when the drop is almost spherical. Additionally, the major axis of the ellipsoid has a non-zero angle with the observation plane, and consequently L cannot be measured directly. They measured B and calculated L, assuming axisymmetry of the ellipsoid and volume conservation ($L = 8R_0^3/B^2$).

In addition to the factors mentioned earlier, an additional difficulty with the DDR concerns stress relaxation. The drop (or the fibers in the BT and IFR methods) and the matrix phase are assumed to be stress and orientation free. This can be accomplished by annealing the samples slightly above T_g before the experiment. However, since the drop in the conventional DDR is deformed by an external shear force during the experiment, it is risky to assume that the residual stress formed during deforming step disappears completely, especially in systems that have long relaxation times.

In this report, an improved experimental technique is introduced to overcome these difficulties. This method combines the analytical power of the DDR with experimental simplicity of the IFRM. Basically, our method is based on the DDR method, but with our experimental technique, it is possible to deform the drop axisymmetrically ($B = W$) and to orient the drop parallel to the observation plane without any residual stress. We first run the procedure for the interfacial tension measurement by IFR. By analyzing the shape of the retracting fiber, we find that there is a two-stage process. In the first stage, the fiber retracts as described by Carriere, the length shrinks as the diameter grows but the shape remains cylindrical. However, we find a second stage, in which the fiber transforms into an axisymmetric ellipsoid. We then analyze the relaxation from the ellipsoid to extract the interfacial tension. We observed the relaxation of the ellipsoid can be well described in Eq. (1). We call our method the improved deformed droplet retraction (IDDR).

As the kinetics is inversely proportional to a characteristic droplet length scale, bigger initial drops (or fibers) are more desirable. However, as the size of the drop used increases and becomes compatible to the distance between the glass slides, the hydrodynamic interaction between the drop and the glass wall may not be negligible. Hence, we additionally examined the effects that occur when the drop size is comparable to the cell gap width. These experiments were also motivated by recent experiment by Migler [26] who showed that the capillary wave instability is suppressed by the confinement.

2. Experimental

2.1. Materials

Two polymers are used in this study. Polyamide-6 (PA-6) was purchased from Polysciences Inc. (trade name $M_n = 16\,000$)[1]. Polystyrene (PS) was donated from Dow Chemicals (trade name: Styron 666D).[1]

2.2. Rheological measurement

Zero-shear viscosity is critical to get an exact interfacial tension in the dynamic method. They were obtained by measuring the shear viscosity at various shear rate (10^{-2} to $5\ ^{-1}$) in the steady mode. The polymers used in this study show a Newtonian regime at the shear rate of 10^{-2} to $10^{-1}\ s^{-1}$. The rheometer used was an advanced rheometric expansion system.[1] A parallel plate configuration (diameter = 25 mm) was used with a gap of about 1.0 mm. The temperature for the measurement was 230 °C. Measured zero-shear viscosities of PA-6 and PS were 300 and 1200 Pa s, respectively.

2.3. Measurement of interfacial tension

The interfacial tension between PA-6 and PS was measured by three methods: first the IFR, then the IDDR (our method) and finally the DDR. Pellets of PA-6 and PS were dried in a vacuum oven at 80 °C overnight prior to molding and drawing. Disks of PS in 1 mm thickness and 25 mm diameter were pressed between two metal plates on a Carver laboratory press at 180 °C. The PA-6 fibers were obtained by drawing from molten pellets at 230 °C. Diameter ranged from 100 to 300 μm. The fibers were cut with 20 mm length and annealed at 80 °C for about 24 h in a

[1] Certain equipment, instruments or materials are identified in this paper in order to adequately specify the experimental details. Such identification does not imply recommendation by the National Institute of Standards and Technology nor does it imply the materials are necessarily the best available for the purpose.

vacuum oven prior to cutting to a short fiber ranging from 0.5 to 3 mm in length. During the drawing procedure, special care is taken to prevent the absorption of the moisture into the PA-6 fiber. The PA-6 fibers are stored in a vacuum oven at 50 °C to avoid further absorption of moisture. We only use any PA-6 threads which have been stored less than 1 week to avoid deterioration of the sample. An optical shearing system (model Linkam CSS 450)[1] connected to a super VHS videocassette recorder and to a Zeiss transmission optical microscope was used. This device enables the sample to be sheared and heated simultaneously whilst under microscopic observation.

We performed the three different interfacial tension measurements on the same PS–PA sample by employing the following protocol. The short fiber of PA-6 is placed between two films of PS. This sandwiched sample was placed in the shearing device under the microscope. At first, the temperature was elevated and maintained at 200 °C for 10 min in order to ensure perfect imbedding without any undesired deformation of the PA-6 fiber ($T_m = 216$ °C). The gap between the two glass walls was then adjusted very slowly to the desired size ranging from 0.5 to 2.5 mm. The temperate was then increased to 230 °C. To perform measurements, images from the microscope were recorded onto video-tape. In stage I, the fiber is described as a retracting cylinder capped with two hemispheres and we used the Carriere and co-workers [13–15] method to extract interfacial tension (IFR). In stage II, the later stage of retraction, it was observed that the short fiber transforms to a perfect axisymmetric ellipsoid. Thus, the images captured at a later stage of the whole retraction process were used to calculate interfacial tension by DDR. This is the IDDR method. After an IFR was completed, the equilibrium spherical drop was deformed by the applied shear force. Typical applied shear rates applied were 0.05–0.2 s^{-1} for about 10 s. The images during the subsequent retraction process were then recorded. Thus we also obtained and analyzed the data for interfacial tension via conventional DDR.

3. Results and discussions

Fig. 1 is a typical set of optical micrographs for the retraction of PA-6 in the PS matrix at 230 °C, whereby an initial cylindrical fiber transforms gradually into a sphere. In stage I of this process ($t < 100$ s), the relaxation is described by IFR. In stage II ($t > 100$ s), the shape of the PA-6 is ellipsoidal, implying that the shape evolution can then be described in Eq. (1) rather than the equation for the IFR. In this stage, the drop shape is an axisymmetrical ellipsoid because it was transformed from an axisymmetrical cylinder under neither pressure nor external force. It is also expected that the major axis of the ellipsoid has zero angle with the observation plane because the axis of the original fiber was parallel to the observation plane. This is confirmed by the

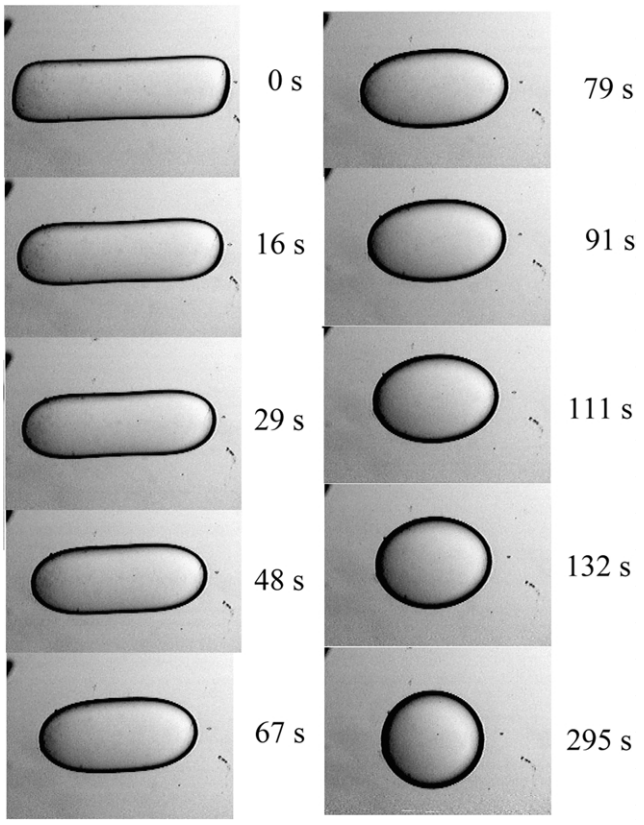

Fig. 1. A typical optical micrograph of the short fiber retraction of PA-6 immersed in a PS matrix. An equilibrium diameter, $2R_0$, of the droplet is 285 μm. A size of the gap containing a PS matrix is 1200 μm.

observation that both tips of the deformed drop are in clear focus in the microscope.

In Fig. 2, the experimental contours of a typical drop at stage II of the retraction process are compared to the calculated ellipse. It is seen that the calculated ellipse becomes coincident with the experimental contour as time increases,

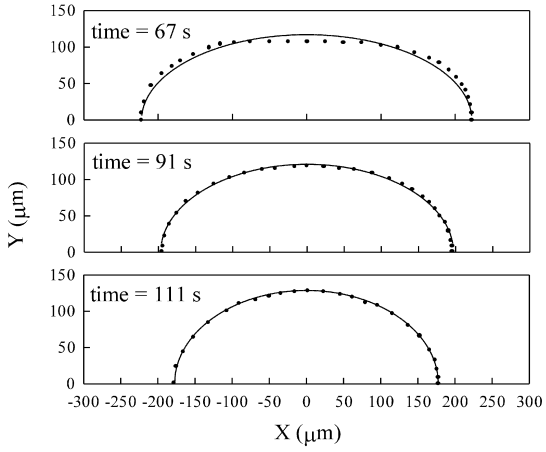

Fig. 2. Comparison of experimental contours and equivalent ellipses at various times for the same experiment as in Fig. 1. Relative standard uncertainties are less than 1%.

which means that IDDR can be well applied to the DDR method with Eq. (1).

Fig. 3 shows a plot of $\ln(D)$ as well as the apparent dimensionless volume of the drop versus time at 230 °C. The apparent dimensionless volume is defined as $\pi LB^2/6$ divided by the volume of the equilibrium sphere, $4\pi R_0^3/3$. Here, L and B were measured from the micrographs of PA-6 during the retraction. At the early stage of the retraction process, the apparent dimensionless volume was underestimated compared with the actual volume. This is because the initial shape of the PA-6 phase is not ellipsoidal during stage I. However, as indicated in Fig. 2, the shape of the PA-6 phase becomes a perfect ellipsoid after about 100 s. The apparent volume becomes 1 and constant after about 100 s, which demonstrates the ellipsoidal shape. The plot of $\ln(D)$ versus time shows a straight line after about 100 s with a slope from which σ was estimated by Eq. (1).

Carriere et al. [13] modeled a short fiber as a cylinder capped with two hemispheres, and expressed its shape evolution when it is imbedded in another polymer liquid as follows:

$$f\left(\frac{R}{R_0}\right) - f\left(\frac{R_e}{R_0}\right) = \frac{2.7}{(1.7p+1)}\frac{\sigma}{\eta_m R_0}t \tag{2}$$

where R_e is an equilibrium drop radius and

$$f(x) = \frac{3}{2}\ln\frac{\sqrt{1+x+x^2}}{1-x} + \frac{3^{1.5}}{2}\arctan\left(\sqrt{3}\frac{x}{2+x}\right) - \frac{x}{2} - \frac{4}{x^2} \tag{3}$$

The other variables are the same as those shown in Eq. (1). Fig. 4 is a typical plot of $f(R/R_0) - f(R_e/R_0)$ versus retraction time. The interfacial tension was determined from the slope of the curve by Eqs. (2) and (3) [13]. We see that the initial period of the retraction (stage I) is linear, but the data deviates from linearity in stage II when the shape of initially imbedded short fiber becomes ellipsoidal. We took this initial slope to calculate the interfacial tension by IFR and the value was compared with the value obtained by the IDDR. The result will be shown and discussed in later section.

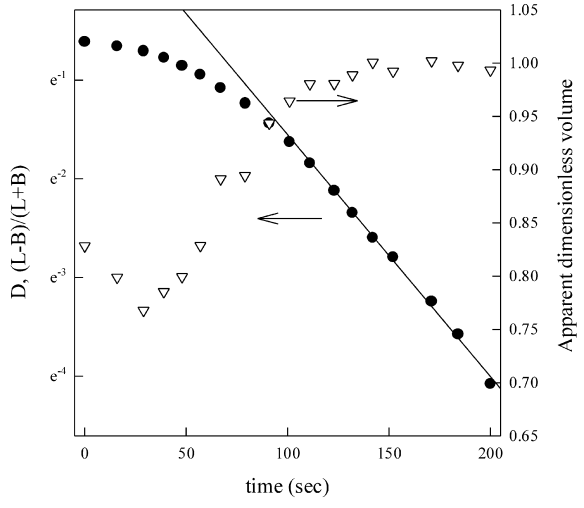

Fig. 3. Time evolution of deformability D and the dimensionless calculated volume for a PA-6 drop immersed in a PS matrix for the same experiment as in Fig. 1. Relative standard uncertainties are less than 1% in apparent dimensionless volume and at most 3% at around 200 s in D.

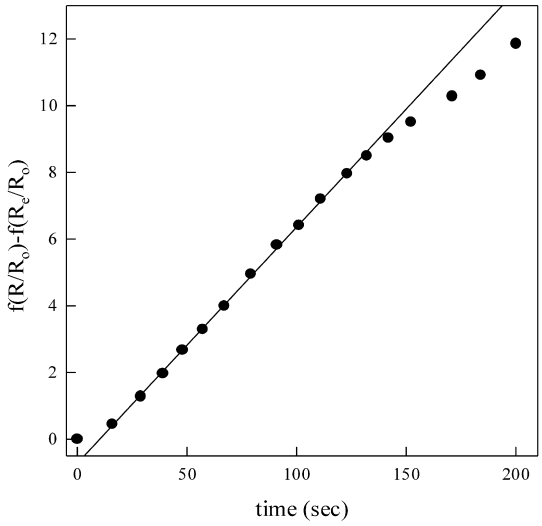

Fig. 4. A typical plot of $f(R/R_0) - f(R_e/R_0)$ versus retraction time matrix for the same experiment as in Fig. 1. Relative standard uncertainties are less than 2%.

The interfacial tension, obtained by IDDR, was compared to that obtained by the conventional DDR. Fig. 5 is a typical optical micrograph for the retraction process of a PA-6 drop initially deformed by external shear flow. The applied shear rate was about 0.06 s^{-1} for about 10 s which corresponds to capillary number ($\gamma\eta_m 2R_0/\sigma$) of 3.2. All drops shown in Fig. 5 seem to be ellipsoidal in the plane of observation. However, we cannot be sure that the drops are axisymmetrical. Furthermore, it is obvious that the major axis is not parallel to the observation plane since the two tips of the drop, especially at the beginning of the experiment, were observed to be out of focus with each other. In Fig. 6, the deformation and apparent dimensionless volume are plotted with respect to time. Here, L for the calculation of the volume was directly measured from the photograph (which approximately corresponds to the real L multiplied by $\cos(\theta)$, where θ is an orientation angle) and L for the calculation of deformation was calculated by volume conservation, i.e. $L = 8R_0/B^2$. The apparent dimensionless volume at $t < 20$ s is greater than 1, meaning that the length of the observed minor axis is bigger than that of the other minor axis, *thus the drop is not axisymmetric*. The apparent volume decreases rapidly to a minimum and then gradually increases to the equilibrium value. A plot of $\ln(D)$ versus time shows a linear relationship after this minimum of apparent volume. It is seen that the data points are more scattered from the linear line compared to that by IDDR, especially at the low value of deformation. This is because

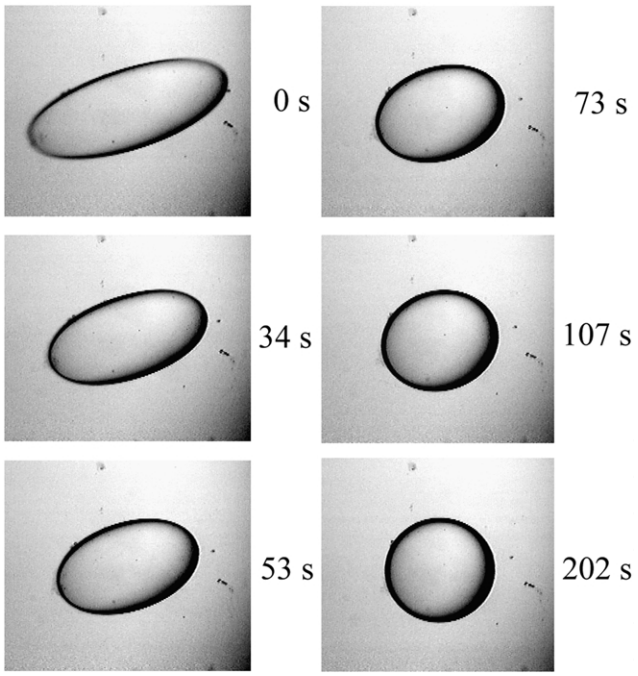

Fig. 5. Optical micrograph of the retraction process for the ellipsoidal drop initially deformed by an external shear force. The applied shear rate was about 0.06 s^{-1}. The other conditions are the same as in Fig. 1.

the major axis, L, was calculated by volume conservation which may give a somewhat higher error in the measurement of interfacial tension than direct measurement of L.

Fig. 7 shows the interfacial tension values measured by the three methods: IFR, DDR and IDDR. The data is plotted as a function of wall gap/equilibrium drop diameter ratio. The data points with error bars represent average values from the data points taken at ratios larger than 2. The interfacial tension measured by the DDR and IFR methods were

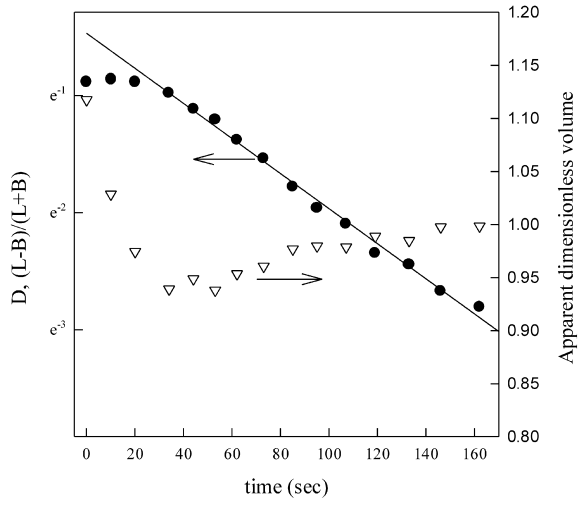

Fig. 6. Time evolution of deformability D and the dimensionless calculated volume for the same experiment as in Fig. 5. Relative standard uncertainties are less than 1% in apparent dimensionless volume and at most 3% at around 160 s in D.

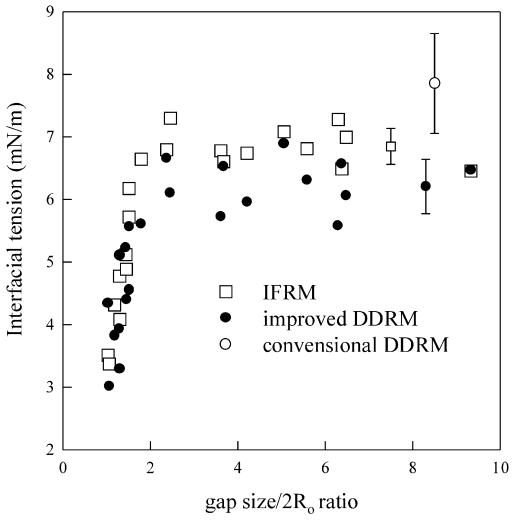

Fig. 7. Interfacial tension obtained in this study versus the gap size/equilibrium drop diameter ratio.

found to be much affected by the gap/drop size ratio. The interfacial tension increased rapidly to the unperturbed value with the ratio. The interfacial tension value above the ratio of 2 is constant regardless of the gap/drop size ratio. It is expected that the rate of shape evolution is hindered by the wall as the drop size increases. However, it is somewhat surprising that the ratio at which the wall begins to affect the rate of the shape evolution is quite small. It is probably because the effect of the wall is only one-dimensional. It is expected that the rate is more hindered in the situation that drop is confined to a circular or rectangular duct.

Fig. 8 is plot of ln(D) as well as the apparent dimensionless volume of the drop versus time at the gap/drop size ratio of

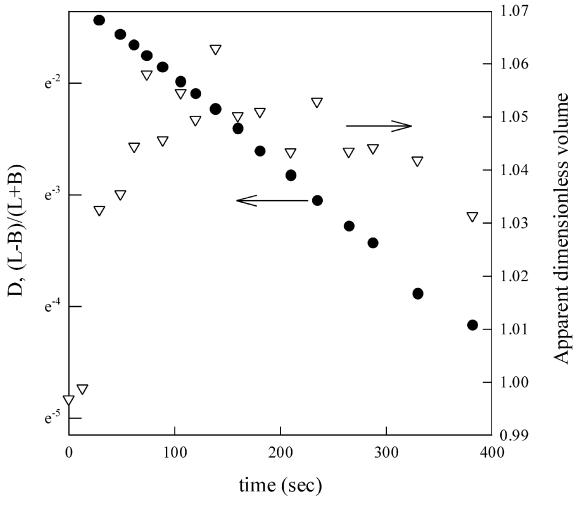

Fig. 8. Time evolution of deformability D and the dimensionless calculated volume for a PA-6 drop immersed in a PS matrix. An equilibrium diameter, $2R_0$, of the droplet is 462 μm. A size of the gap containing a PS matrix is 600 μm. Relative standard uncertainties are less than 1% in apparent dimensionless volume and at most 3% at around 400 s in D.

1.3. Contrary to the trend presented in Fig. 3 (unperturbed result), the apparent volume exceeds the equilibrium value for $t > 20$ s. It was observed that the shape of the drop projected to the observation plane was ellipsoidal during this period. This implies that the initially axisymmetrical short fiber transforms to a flattened ellipsoid at a later stage of the retraction process. This is probably because the lateral expansion of the drop towards the wall direction is suppressed by hydrodynamic interactions between the drop and the wall.

The interfacial tension values measured by IDDR were slightly lower than those measured by either the IFR or the DDR. The variation is in an acceptable range. The differences in interfacial tension between DDR and IDDR could arise from a systematic error in determining L and/or the residual stress caused by external shear stress. In all dynamic methods, the driving force to the equilibrium shape is assumed to be purely interfacial. Therefore, residual stress may cause the droplet to relax faster, yielding an interfacial tension value that is too large [27].

IDDR enables us to use the interfacial force-driven shape recovery of an axisymmetric ellipsoidal drop formed by the retraction of a short fiber. An advantage of this technique over the conventional DDR is that it is possible to measure the interfacial tension of polymer pairs with high viscosity ratio. According to Grace's work [28], when a viscosity of the drop is 3.4 times higher than that of matrix phase, a drop is hardly deformed by the shear force. Therefore, it is difficult to obtain a deformed drop by the conventional technique suggested by Luciani et al. This limitation may be circumvented using extensional stress. However, it is not easy to design experimental equipment using extensional flow.

One advantage of the conventional DDR method is that the experiment can be repeated several times on one sample by deforming a spherical drop again after cessation of one run unless the thermal degradation is serious. IDDR cannot be repeated on the same sample because the deformed drop is formed by the retraction of the short fiber.

4. Conclusion

In this study, axisymmetric ellipsoidal polymer drops are obtained by the retraction of short fibers imbedded in matrix polymer liquids. We observed that imbedded short fibers at a later stage of retraction transform into axisymmetrical ellipsoids. Then, the shape evolution of the drop is described by a well-known equation, which yields the interfacial tension. It is demonstrated that the suggested experimental technique can overcome several limitations encountered in conventional interfacial tension measurements. The interfacial tension values obtained for the PA-6/PS were found to be slightly lower than those obtained by the conventional methods.

We also observed that the shape relaxation decreases as the drop size becomes compatible to the gap width.

References

[1] Paul DR, Newman S. Polymer blends. New York: Academic Press, 1978.
[2] Wu S. Polym Engng Sci 1990;30:753.
[3] Anastasiadis SH, Chen JK, Koberstein JT, Siegel AF, Sohn JE, Emerson JA. J Colloid Interface Sci 1987;119:55.
[4] Demarquette NR, Kamal MR. Polym Engng Sci 1994;34:1823.
[5] Kamal MR, Lai-Fook R, Demarquette NR. Polym Engng Sci 1994;34:1834.
[6] Coucoulas LM, Dawe RA. J Colloid Interface Sci 1985;103:230.
[7] Patterson HT, Hu KH, Grindstaff TH. J Polym Sci Part C 1971;34:31.
[8] Joseph DD, Arney MS, Gillbert G, Hu H, Dulman D, Verdier C, Vinagre TM. J Rheol 1992;36:621.
[9] Elmendorp JJ. Polym Engng Sci 1986;26:418.
[10] Elemans PHM, Janssen JMH, Meijer HEH. J Rheol 1990;34:1311.
[11] Cho K, Jeon HK, Park CE, Kim J, Kim KU. Polymer 1996;37:1117.
[12] Son Y. Polymer 2001;42:1287.
[13] Carriere CJ, Cohen A, Arends CB. J Rheol 1989;33:681.
[14] Cohen A, Carriere CJ. Rheol Acta 1989;28:223.
[15] Carriere CJ, Cohen A. J Rheol 1991;35:205.
[16] Lee YU, Kim HC, Jo WH. Polymer—Korea 1997;21:1066.
[17] Luciani A, Champagne MF, Utracki LA. J Polym Sci Phys Ed 1997;35:1393.
[18] Tomotika S. Proc R Soc Lond 1935;A150:322.
[19] Rallison JM. Annu Rev Fluid Mech 1984;16:45.
[20] Levitt L, Macosko CW, Pearson SD. Polym Engng Sci 1996;36:1647.
[21] Hayashi R, Takahashi M, Yamane H, Jinnai H, Watanabe H. Polymer 2001;42:757.
[22] Yamane H, Takahashi M, Hayashi R, Okamoto K, Kashihara H, Masuda T. J Rheol 1998;42:567.
[23] Guido S, Villone M. J Rheol 1998;42:395.
[24] Migler KB. J Rheol 2000;44:277.
[25] Mighri F, Huneault MA. J Rheol 2001;45:783.
[26] Migler KB. Phys Rev Lett 2001;86:1023.
[27] Xing P, Bousmina M, Rodrigue D. Macromolecules 2000;33:8020.
[28] Grace HP. Chem Engng Commun 1982;14:225.